

***Final Draft***  
**of the original manuscript:**

Guglielmi, P.O.; Herbert, E.G.; Tartivel, L.; Behl, M.; Lendlein, A.;  
Huber, N.; Lilleodden, E.T.:

**Mechanical characterization of oligo(ethylene glycol)-based  
hydrogels by dynamic nanoindentation experiments**

In: Journal of the Mechanical Behavior of Biomedical Materials  
(2015) Elsevier

DOI: 10.1016/j.jmbbm.2015.02.009

1  
2  
3  
4 **Mechanical characterization of oligo(ethylene glycol)-based hydrogels by dynamic**  
5 **nanoindentation experiments**  
6

7 P.O. Guglielmi<sup>a\*</sup>, E.G. Herbert<sup>b</sup>, L. Tartivel<sup>c</sup>, M. Behl<sup>c</sup>, A. Lendlein<sup>c</sup>, N. Huber<sup>a</sup>, and E.T.  
8 Lilleodden<sup>a</sup>  
9

10 <sup>a</sup> Helmholtz-Zentrum Geesthacht, Institute of Materials Research, Materials Mechanics,  
11 21502 Geesthacht, Germany  
12

13 <sup>b</sup> University of Tennessee, Department of Materials Science and Engineering, Knoxville, TN  
14 37917  
15

16 <sup>c</sup> Helmholtz-Zentrum Geesthacht, Institute of Biomaterial Science, 14513 Teltow-Seehof,  
17 Germany  
18  
19  
20

21 **Abstract**  
22

23 Oligo(ethylene glycol)-based hydrogel samples (OEG hydrogels) of varying cross-link  
24 densities and degrees of swelling were characterized through dynamic nanoindentation  
25 testing. Experiments were performed using a non-standard nanoindentation method which  
26 was validated on a standard polystyrene sample. This method maximizes the capability of the  
27 instrument to measure the stiffness and damping of highly compliant, viscoelastic materials.  
28 Experiments were performed over the frequency range of 1 to 50 Hz, using a 1 mm diameter  
29 flat punch indenter. A hydration method was adopted to avoid sample dehydration during  
30 testing. Values of storage modulus ( $E'$ ) ranged from 3.5 to 8.9 MPa for the different OEG-  
31 hydrogel samples investigated. Samples with higher OEG concentrations showed greater  
32 scatter in the modulus measurements and it is attributed to inhomogeneities in these materials.  
33 The  $E'$  values did not show a strong variation over frequency for any of the samples. Values  
34 of loss modulus ( $E''$ ) were two orders of magnitude lower than the storage modulus, resulting  
35 in very low values of loss factor ( $E''/E' < 0.1$ ). These are characteristics of strong gels, which  
36 present negligible viscous properties.  
37  
38  
39  
40  
41  
42  
43  
44  
45  
46  
47  
48  
49  
50  
51  
52  
53  
54

55 **Keywords: nanoindentation, hydrogel, mechanical properties, dynamical testing**  
56

57 \* contact author: [paula.guglielmi@hzg.de](mailto:paula.guglielmi@hzg.de), tel. +49 41 52 87 2547, fax +49 41 52 26 25  
58  
59  
60  
61

62 CSM: constant stiffness measurement; PCM: polymer characterization method; OEG:  
63 oligo(ethylene-glycol);  $E'$ : storage modulus;  $E''$ : loss modulus;  $\tan\delta$ : loss factor  
64  
65

## 1. Introduction

Hydrogels are hydrophilic polymer networks swollen by water or aqueous solutions, which makes them interesting for several biomedical applications that require the material to mimic soft tissues (Hu et al., 2012; Lin and Anseth, 2009; Peppas et al., 2000; Shapiro and Oyen, 2014). As an example, oligo(ethylene glycol)-based hydrogels present characteristics such as non-cytotoxicity, protein repellency, and compatibility with tissues or blood, which created significant interest in exploring their suitability for applications such as controlled drug delivery and regeneration of damaged articular cartilage (Gläber et al., 2009; Lin and Anseth, 2009; Lum and Elisseff, 2003).

When used as tissue replacements, hydrogels are designed to mimic the mechanical behavior of the natural tissue and its response to the complex loading conditions endured by the body (Ahearne et al., 2005; Franke et al., 2007; Franke et al., 2008). In drug or cell delivery applications, mechanical properties are important since the delivery devices must maintain their structural integrity to protect drugs or cells until they are released into the body (Franke et al., 2007). In addition, in applications where gels are used as matrices for stem cells differentiation, it has been reported that the elastic properties of the gels strongly influence the lineage specification of mesenchymal stem cells (Engler et al., 2006). Clearly, the successful biomedical application of hydrogels largely depends on the ability to tune, as well as accurately and precisely characterize their mechanical behavior.

A variety of conventional methods have been used to characterize the mechanical properties of hydrogels. Anseth *et al.* (Anseth et al., 1996) and Peppas *et al.* (Peppas and Merrill, 1977) suggested the use of tensile tests, together with the theory of rubber elasticity, to evaluate the mechanical response of hydrogels. Dynamic Mechanical Analysis (DMA) was used by Cauich-Rodriguez *et al.* (Cauich-Rodriguez et al., 1996) to characterize the viscoelastic properties of hydrogel blends over the frequency range of 0.1 to 50 Hz.

1  
2  
3  
4 Additionally, uniaxial confined or unconfined compression has been extensively used due to  
5  
6 the ease of sample preparation and simple test methodology (Iza et al., 1998; Roberts et al.,  
7  
8 2011; Thomas et al., 2004). While these test methods are among the types needed to  
9  
10 investigate the hydrogels constitutive behavior in the time and frequency domains, the wide  
11  
12 variety also reflects the fact that each technique has limitations. In the case of hydrogels, test  
13  
14 methods can and often do produce unreliable data due to the high compliance and time-  
15  
16 dependent deformation of these materials. Their elastic moduli vary from tens of kPa to a few  
17  
18 MPa, which requires high-resolution load measurements. In addition, difficulties in the  
19  
20 preparation of macroscopic samples (Oyen, 2014), problems with sample fixation during  
21  
22 testing (Hu et al., 2012; Oyen, 2014) and the need for testing these materials in the hydrated  
23  
24 state (Oyen, 2014) present a number of challenges in generating reliable data that can be used  
25  
26 to determine their mechanical behavior (Hu et al., 2012; Oyen, 2013, 2014).  
27  
28  
29

30  
31 Recently, instrumented nanoindentation has arisen as an interesting technique to  
32  
33 characterize the mechanical properties and viscoelastic behavior of soft materials such as  
34  
35 polymers, gels and biological tissues (Deuschle, 2008; Ebenstein and Pruitt, 2004, 2006;  
36  
37 Franke et al., 2007; Herbert et al., 2009; Herbert et al., 2008; Kaufman and Klapperich, 2009;  
38  
39 Kaufman et al., 2008; Liu et al., 2009; Oyen, 2006; Oyen and Cook, 2009). In this technique,  
40  
41 a sample is locally compressed by an indenter with known geometry, while load,  
42  
43 displacement and time are constantly recorded and then used to calculate materials properties  
44  
45 (Oyen, 2014). Advantages of using nanoindentation include (i) the ability of testing small  
46  
47 volumes of materials with spatial resolution in the nm to  $\mu\text{m}$  range, enabling the  
48  
49 characterization of heterogeneities typical for biological materials (Deuschle, 2008; Ebenstein  
50  
51 and Pruitt, 2004, 2006; Franke et al., 2007; Herbert et al., 2009; Herbert et al., 2008; Oyen,  
52  
53 2014; Oyen and Cook, 2009; White et al., 2005), (ii) the ability to control and/or measure  
54  
55 very low forces (sub- $\mu\text{N}$ ), displacements (sub-nm) and changes in stiffness ( $<1\text{ N/m}$ ), which  
56  
57 are crucial for testing compliant samples (Deuschle, 2008; White et al., 2005), (iii) the  
58  
59  
60  
61  
62  
63  
64  
65

1  
2  
3  
4 avoidance of extensive macroscopic sample preparation (Oyen, 2014) (Oyen, 2014; Oyen and  
5  
6 Cook, 2009; White et al., 2005) and (iv) the possibility to characterize materials in a variety of  
7  
8 different deformation modes by changing the time scale, indenter tip geometry and loading  
9  
10 conditions (Oyen and Cook, 2009). Additionally, recent developments make it possible to  
11  
12 perform nanoindentation experiments on samples fully submersed in a liquid (Franke et al.,  
13  
14 2011; Hu et al., 2012; Nayar et al., 2012).

15  
16  
17 Like all testing techniques, however, nanoindentation has its limitations. Since it was  
18  
19 primarily developed to test elastic and elasto-plastic materials (Oliver and Pharr, 2004) (which  
20  
21 are much harder than gels), the application of this technique to characterize soft samples  
22  
23 offers unique challenges, and requires adaptation of standard testing procedures. In particular,  
24  
25 surface detection is a critical problem in testing highly compliant materials. Especially when  
26  
27 indenters of varying cross-section are used (such as pyramids and spheres), the point of first  
28  
29 contact between the indenter and the sample must be correctly determined, since the contact  
30  
31 area as a function of contact depth is needed for the calculation of elastic modulus and  
32  
33 hardness. In standard nanoindentation methods, initial contact is usually identified as the point  
34  
35 when a small increase in force or stiffness is detected. Although this works well for hard  
36  
37 materials such as metals or ceramics, even small forces can lead to extensive displacements in  
38  
39 soft materials, thereby leading to zero-point errors and, consequently, to wrong  
40  
41 determinations of contact area and material properties (Kaufman and Klapperich, 2009; Oyen,  
42  
43 2013). Furthermore, the large displacements usually imposed during mechanical loading of  
44  
45 compliant materials require the tip area function to be calibrated for large indentation depths.  
46  
47 This requires reliable reference materials characterized by a similar compliance as the  
48  
49 samples to be tested (Kaufman et al., 2008). Apart from these “extrinsic effects”, the intrinsic  
50  
51 time-dependent deformation of hydrogels and how it can be characterized using  
52  
53 nanoindentation is also an experimental challenge (Ebenstein and Pruitt, 2004; Franke et al.,  
54  
55 2008; Kaufman and Klapperich, 2009; Oyen and Cook, 2009; Shapiro and Oyen, 2014).  
56  
57  
58  
59  
60  
61  
62  
63  
64  
65

1  
2  
3  
4 Time-dependent deformation of hydrogels results from a combined effect of the  
5  
6 intrinsic viscoelasticity of the polymer matrix and the poroelasticity associated with the flow  
7  
8 of a liquid through the porous polymeric network (Hu et al., 2012; Oyen, 2013, 2014).  
9  
10 Nanoindentation data is therefore normally analyzed using viscoelastic or poroelastic models  
11  
12 (Galli et al., 2008; Hu et al., 2012; Kaufman et al., 2008; Oyen et al., 2007; Shapiro and Oyen,  
13  
14 2014), being most experiments performed in the time domain, i.e. by creep or stress-  
15  
16 relaxation tests (Galli et al., 2008; Hu et al., 2012; Kaufman et al., 2008; Oyen, 2007; Shapiro  
17  
18 and Oyen, 2014). Nevertheless, for applications such as articular cartilage regeneration, the  
19  
20 investigation of material properties in the frequency domain is also of great interest, since  
21  
22 such soft tissues are daily submitted to a wide range of frequencies during regular walking  
23  
24 (Franke et al., 2008). To date, however, only a few works have been reported on the dynamic  
25  
26 characterization of gels by instrumented indentation (Nayar et al., 2012; Tyrrel and Attard,  
27  
28 2003).  
29  
30  
31  
32

33  
34 This work aims to characterize the mechanical properties of OEG hydrogels in the  
35  
36 frequency domain. Therefore, a dynamic nanoindentation routine is emphasized and the data  
37  
38 is analyzed on the basis of linear viscoelasticity. When a sinusoidal load is applied to a  
39  
40 viscoelastic material, the response is a deformation function of the same frequency, but one  
41  
42 which lags behind the loading function by a phase  $\delta$ . In this context, indentation tests are  
43  
44 performed here using the so-called continuous stiffness measurement (CSM) technique, in  
45  
46 which a sinusoidal load is applied to the material and the resulting harmonic displacement and  
47  
48 phase angle are measured (Oliver and Pharr, 1992). This enables measurement of the loss  
49  
50 factor ( $\tan\delta$ ) and, assuming the contact area is known or can be determined, then the storage  
51  
52 and loss moduli ( $E'$  and  $E''$ , respectively) can be measured as well (Herbert et al., 2009;  
53  
54 Herbert et al., 2008; White et al., 2005). The experimental method used in this study is based  
55  
56 on previous works reported by Herbert *et al.* (Herbert et al., 2009; Herbert et al., 2008), in  
57  
58 which a meaningful methodology to accurately characterize the viscoelastic properties of soft  
59  
60  
61  
62  
63  
64  
65

1  
2  
3  
4 polymers using dynamic nanoindentation is presented. Advantages of this methodology  
5  
6 include an accurate method to determine the point of first contact between indenter and  
7  
8 sample based on the measured phase angle, and the use of a right cylindrical flat punch with a  
9  
10 constant cross-section in order to minimize errors associated with the contact area calculation.  
11  
12 A hydration method is used to avoid excessive drying of the samples during testing. Both  
13  
14 polymer concentration and OEG molecular weight were varied, resulting in gels with different  
15  
16 cross-link densities and degrees of swelling. Apart from evaluating the influence of these  
17  
18 parameters in the final mechanical properties of the materials, this work aims at evaluating the  
19  
20 applicability of the CSM technique to discriminate between soft materials with slightly  
21  
22 different mechanical properties.  
23  
24  
25  
26

## 27 **2. Materials and methods**

### 28 *2.1 Sample preparation*

29  
30  
31  
32  
33 OEG hydrogels were prepared from dimethacrylate or diacrylate terminated  
34  
35 oligo(ethylene glycol)s. These compounds (OEGDMA,  $M_w = 1000$  g/mol from Polysciences,  
36  
37 USA or  $M_w = 750$  g/mol Sigma-Aldrich, Germany and OEGDA,  $M_w = 700$  g/mol from  
38  
39 Sigma-Aldrich, Germany) were dissolved in water in different concentrations. Benzophenone  
40  
41 (BP, Sigma-Aldrich, Germany) was used as photoinitiator in a quantity of 0.01 g (0.05 mmol).  
42  
43  
44 In order to remove oxygen, which acts as a free radical scavenger, nitrogen was bubbled  
45  
46 through the reaction mixture for 15 min. Hydrogel plates were prepared by pouring the  
47  
48 reaction mixture into Petri dishes, and exposing them to the UV light of a mercury lamp (type  
49  
50 FUSION) for 1 h at 10°C. Upon completion, the hydrogel plates were removed and washed in  
51  
52 distilled/deionized water for 1 week to remove unreacted precursor or initiator. After washing,  
53  
54 the samples were stored in water to reach equilibrium swelling. Three different hydrogel  
55  
56 samples were analyzed in this study, which are identified in Table 1. They varied in the  
57  
58 amount of solvent and molecular weight of the OEG-compound used. Values of gel content  
59  
60  
61  
62  
63  
64  
65

1  
2  
3  
4 obtained in synthesis ranged between 98% and 100% (statistical values), indicating a high  
5  
6 degree of cross-linking. For the nanoindentation experiments, the hydrogel plates (~5 cm  
7  
8 diameter and 0.5 to 0.7 cm height) were cut into small samples of ~1 cm<sup>2</sup> using a razor blade.  
9  
10 A hydration method reported by Kaufman and Klapperich (Kaufman and Klapperich, 2009)  
11  
12 was used to keep the hydrogel samples hydrated during the nanoindentation experiments. In  
13  
14 this method, the gels are fixed to a glass slide using a small droplet of cyanoacrylate glue. The  
15  
16 sample is then encircled with a hydrophobic barrier pen, ImmEdge™ Pen (Vector  
17  
18 Laboratories, USA) and the small circle carefully filled with water. In reference  
19  
20 measurements, no influence of the cyanoacrylate glue on the mechanical properties of the gels  
21  
22 was observed. Moreover, since this method only keeps samples laterally hydrated, no more  
23  
24 than two indents were performed per small sample, in order to avoid excessive drying of the  
25  
26 gels surface.  
27  
28  
29  
30  
31

32  
33 **Table 1:** oligo(ethylene glycol)-based hydrogel samples analyzed in this work.

34 <b>Sample Code</b>	35 <b>Compound/solvent ratio (wt%)</b>	36 <b>OEG-compound</b>	37 <b>OEG-compound molecular weight (g/mol)</b>
38 H50/1000	39 50	40 OEGDMA	41 1000
42 H50/750	43 50	44 OEGDMA	45 750
46 H30/700	47 30	48 OEGDA	49 700

50  
51 In addition to the hydrogels, a polystyrene (PS) reference sample ( $M_w = 250000$  g/mol,  
52  
53 Acros Organics, Belgium) was investigated in the early part of this work to establish and  
54  
55 further validate the testing protocol. PS is a suitable reference material, since it is an  
56  
57 amorphous thermoplastic with a glass transition temperature of ~95°C and a surface which is  
58  
59 generally free of contaminants.  
60  
61

## 62 2.2 Experimental methods

63  
64 Nanoindentation experiments were performed using a Nanoindenter<sup>®</sup> XP (Agilent  
65  
Technologies, USA) and a modified CSM method, which we will refer to as “*Polymer*



1  
2  
3  
4 *Characterization Method*” (PCM). In this method, a frequency sweep is used to characterize  
5  
6 the samples over the frequency range of 1 to 50 Hz. More details on this test methodology are  
7  
8 given in the next section. Hydrogel samples were tested using a large stainless steel right  
9  
10 cylindrical flat punch (1 mm in diameter), in order to establish sufficient contact stiffness.  
11  
12 Since hydrogels are very compliant materials, it is important to increase the contact area so  
13  
14 that the exerted forces are in the indenter working range (Oyen, 2013). The PS reference  
15  
16 sample is, in turn, much stiffer than the gels and could be tested using a 50  $\mu\text{m}$  flat punch.  
17  
18

19  
20 For the sake of comparison, tests on PS were also conducted using a standard CSM  
21  
22 method (readily available within the instrument software) over the frequency range of 4 to 45  
23  
24 Hz. In this case, experiments were performed using both a sharp Berkovich indenter and a 50  
25  
26  $\mu\text{m}$  diameter flat punch, using a harmonic displacement of 50 nm.  
27  
28

29  
30 In order to compare the results from our nanoindentation experiments with those of a  
31  
32 conventional unconfined uniaxial compression method, tests on hydrogels were performed  
33  
34 according to the test standard DIN 53421/ISO 844, using a Zwick/Roell machine. Samples  
35  
36 with 21 mm diameter and  $\sim 7.5$  mm height were compressed at a displacement rate of 2  
37  
38 mm/min (or equivalent strain rate of  $\sim 0.004/\text{s}$ ) until 50% of deformation. A pre-load of 0.1 N  
39  
40 was used in all tests. The elastic modulus was measured as the slope of the stress-strain curve  
41  
42 at 1 N of applied force ( $\sim 3$  kPa and 2% strain for these samples).  
43  
44

## 45 46 *2.2 The polymer characterization method (PCM)* 47

48  
49 In the PCM method, the indentation system, together with the tip-sample contact, is  
50  
51 modeled as a simple harmonic oscillator, in which sample and instrument are connected in  
52  
53 parallel, since they undergo the same change in displacement. The sample is assumed to  
54  
55 behave as a viscoelastic Kelvin-Voigt solid, modeled by a spring and a dashpot in parallel.  
56  
57 The spring represents the instantaneous elastic contribution to deformation, while the dashpot  
58  
59 (damper) is associated with the time-dependent, viscous properties of the material. The raw  
60  
61  
62  
63  
64  
65

1  
2  
3  
4 output of an experiment in the frequency domain, when instrument and contact endure steady-  
5  
6 state harmonic motion, is a combined frequency response of the instrument and the sample.  
7  
8 Therefore, the use of dynamic nanoindentation to characterize viscoelastic properties of  
9  
10 materials relies on the ability to accurately characterize the stiffness and damping of the  
11  
12 measuring instrument itself, so that the response of the sample can be correctly isolated from  
13  
14 the total measured response (Herbert et al., 2008). Additionally, the data must be  
15  
16 representative of steady-state harmonic motion, a known contact geometry, and linear  
17  
18 viscoelasticity (Herbert et al., 2009; Herbert et al., 2008). More details on the theory  
19  
20 underlying this characterization method, as well as on the methodology used are found in  
21  
22 (Herbert et al., 2008) and will be only briefly described here.  
23  
24  
25

26  
27 The load-time history of the PCM method is shown in Fig. 1(a). The experiment starts  
28  
29 with the surface finding, indicated in Fig. 1(a) by number (1). To accurately determine the  
30  
31 point of first contact between sample and indenter tip, the phase shift between the applied  
32  
33 harmonic load and the resulting harmonic displacement is constantly monitored, while the  
34  
35 indenter tip slowly approaches the sample surface at  $10 \mu\text{N/s}$  with a frequency of 50 Hz. The  
36  
37 first contact between indenter tip and sample surface is associated with an abrupt change in  
38  
39 the measured phase shift. This change is related to the difference in the dynamic response of  
40  
41 the instrument itself (i.e., the indenter hanging in air) and that when the tip is in contact with  
42  
43 the sample. According to Herbert *et al.* (Herbert et al., 2008), the change in harmonic  
44  
45 displacement is also a good indicator for the surface finding. When the point of first contact is  
46  
47 achieved, the values of displacement into the surface and the load on the sample are zeroed  
48  
49 and the experimental loading protocol commences.  
50  
51  
52

53  
54 After surface contact is established, full contact of the flat punch must be achieved,  
55  
56 such that the contact diameter is equal to the punch diameter. This is established by applying a  
57  
58 pre-load at  $250 \mu\text{N/s}$  while constantly monitoring the harmonic displacement at a frequency  
59  
60 of 50 Hz, as shown by segment 2 of Fig. 1(a). Full contact is indicated when the harmonic  
61  
62  
63  
64  
65

displacement or dynamic stiffness stabilizes at a constant value. After achieving full contact, the sample continues to be loaded at 250  $\mu\text{N/s}$ , until a prescribed depth limit is achieved. In case of the PS sample, a depth limit of 5  $\mu\text{m}$  was used. Due to the high compliance of the hydrogels, however, full contact between the punch and the sample was achieved only at large displacements; depth limits on the order of 40  $\mu\text{m}$  were required.

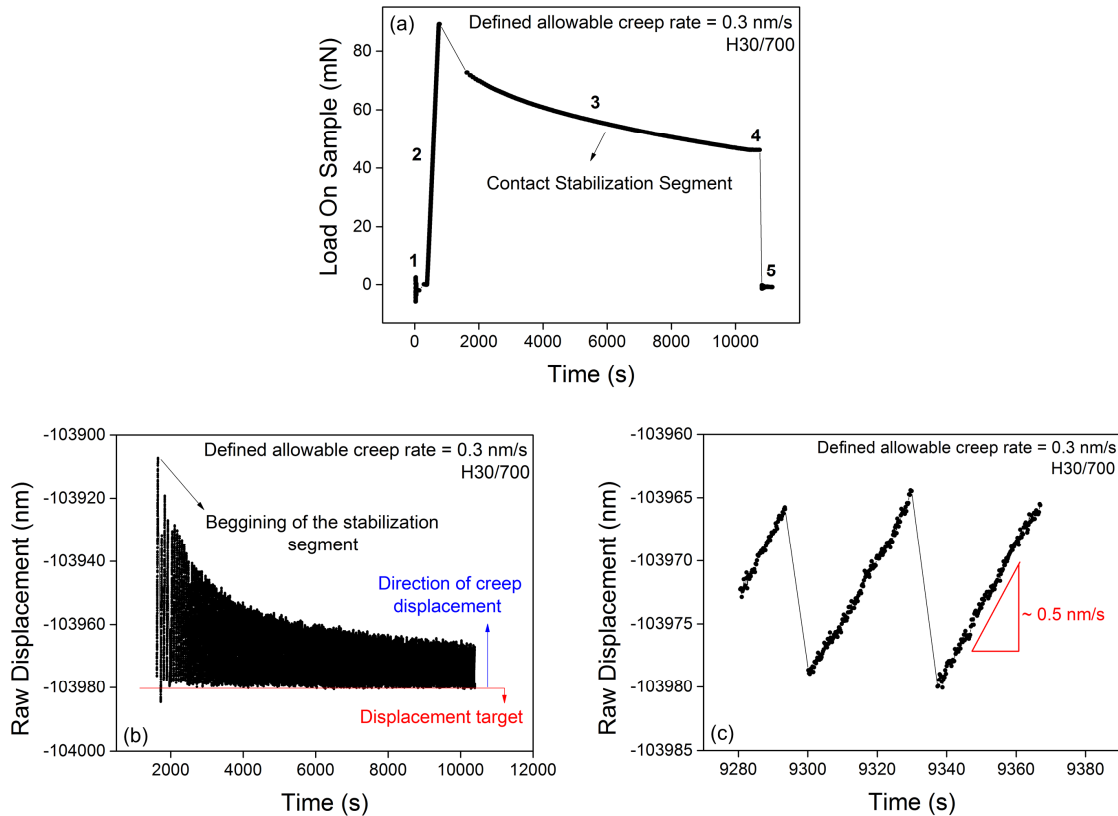


**Fig. 1:** (a) Load-time history of a nanoindentation experiment performed on a H30/700. (b) Raw displacement as a function of time related to the contact stabilization segment of the method for an experiment performed with 0.3 nm/s of allowable creep rate. (c) Closer look on data shown in (b), showing the creep rate after approx. 2.5 h of experiment.

The next step in the loading protocol is the “contact stabilization segment”, as indicated by segment (3) in Fig. 1(a). In order for the combined frequency response of the instrument and the sample to be accurately modeled as a simple harmonic oscillator, transient behavior (i.e., creep, in case of load-controlled experiments) must be given enough time to stabilize, such that its effects on the dynamic response is negligible (Herbert et al., 2008). This test segment aims therefore at stabilizing the creep behavior of the sample, so that (i) steady-

1  
2  
3  
4 state harmonic motion can be achieved and (ii) the imposed strains are consistent from one  
5  
6 experiment to the next and are, ideally, within the linear viscoelastic limit. For that, once the  
7  
8 prescribed depth limit is reached, the load is kept constant and the creep rate is monitored  
9  
10 over a 30 s interval. The measured rate is then compared to a prescribed stabilization criterion  
11  
12 (e.g. 0.3 nm/s). If the measured value is higher than this criterion, the load is reduced at  $\sim 10$   
13  
14  $\mu\text{N/s}$ , until the indenter comes back to the raw displacement associated to the prescribed depth  
15  
16 limit, the so-called “displacement target” as indicated in Fig. 1(b) by the red line. At this  
17  
18 point, the load is held constant again and the sample is allowed to creep for a new creep rate  
19  
20 measurement, as indicated in Fig. 1(b) by the blue arrow. This routine continues until the  
21  
22 allowable creep rate criterion is met.  
23  
24  
25

26  
27 After the creep behavior is settled, the dynamic characterization of the system  
28  
29 (combined response of instrument and sample) starts, indicated by number (4) in Fig. 1(a).  
30  
31 This characterization was performed at frequencies of 1, 3, 5, 10, 20, 30, 40 and 50 Hz, with a  
32  
33 displacement amplitude of 50 nm.  
34  
35

36  
37 The last segment in the experiment (number (5) in Fig. 1(a)) is the characterization of  
38  
39 the dynamic response of the measurement instrument itself, so that the sample’s response can  
40  
41 accurately be isolated from the values measured in segment (4). This is done with the indenter  
42  
43 hanging in air, which is why the load on sample is near 0 mN. Because the dynamic stiffness  
44  
45 and damping of the Nanoindenter<sup>®</sup> XP are not only a function of frequency, but also depend  
46  
47 on the physical location of the indenter shaft in relation to the capacitance gauge used to  
48  
49 measure displacements (Herbert et al., 2008), the characterization of the instrument in free  
50  
51 space was conducted for each single experiment at the same position where the contact was  
52  
53 characterized. The instrument’s response was then measured at the same frequencies used in  
54  
55 the dynamic measurements of the contact, but using a displacement amplitude of 5000 nm.  
56  
57  
58 The fact that the instrument’s dynamic response was characterized for each single experiment  
59  
60  
61  
62  
63  
64  
65

1  
2  
3  
4 significantly increases the accuracy with which the viscoelastic properties of the sample are  
5  
6 isolated from the system dynamic response.  
7  
8

### 9 10 2.3 Fundamentals of dynamic contact

11  
12 In the limit of linear viscoelasticity, the elastic-viscoelastic principle is valid, so that  
13  
14 Sneddon's stiffness equation (the fundamental equation of nanoindentation) may be used to  
15  
16 relate the dynamic stiffness and damping of the contact to the storage ( $E'$ ) and loss modulus  
17  
18 ( $E''$ ) of the material (Herbert et al., 2009; Herbert et al., 2008). The storage modulus is a  
19  
20 measure of the material's capacity to store energy, as described by the spring in the Kelvin-  
21  
22 Voigt model. The loss modulus is related to the material's capacity to dissipate energy, as is  
23  
24 associated with the dashpot in the viscoelastic model. The ratio between the loss and the  
25  
26 storage moduli (Eq. (3)) is called the loss factor and is normally used as a measure of  
27  
28 damping in a linear viscoelastic material. The higher this value, the more time-dependent  
29  
30 (viscous) the material is and the higher its capacity to dissipate energy.  
31  
32

33  
34  
35 The viscoelastic properties of the hydrogels were calculated from the nanoindentation  
36  
37 data through the following equations:  
38

$$39  
40  
41 E' = (1 - \nu^2) \frac{F_o}{h_o} \cos\delta \frac{\sqrt{\pi}}{2\beta\sqrt{A}} \quad (1)$$

$$42  
43  
44  
45 E'' = (1 - \nu^2) \frac{F_o}{h_o} \sin\delta \frac{\sqrt{\pi}}{2\beta\sqrt{A}} \quad (2)$$

$$46  
47  
48  
49  
50  
51 \tan\delta = \frac{E''}{E'} \quad (3)$$

52  
53  
54 where  $\nu$  is the Poisson's ratio,  $F_o$  is the amplitude of the harmonic load oscillation,  $h_o$  is the  
55  
56 resulting harmonic displacement amplitude,  $\delta$  is the phase angle between the harmonic load  
57  
58 and displacement,  $\beta$  is a term related to the geometry of the contact ( $\beta = 1$  for circular flat  
59  
60  
61  
62  
63  
64  
65

1  
2  
3  
4 punch) and  $A$  is the projected contact area. Details about the derivation of these equations can  
5  
6 be found in (Herbert et al., 2009; Herbert et al., 2008).  
7  
8

### 9 **3. Results**

#### 10 *3.1 Validation experiments on polystyrene (PS)*

11  
12  
13  
14  
15 Results of storage modulus from all experiments performed on the PS reference  
16  
17 sample are shown in Fig. 2. Each data point is the average of 10 measurements. While the  
18  
19 results from the standard CSM experiments show poor reproducibility at low frequencies,  
20  
21 values measured with the PCM method present very small standard deviations for all  
22  
23 frequencies. Good agreement between both methods is only achieved at higher frequencies  
24  
25 ( $>20$  Hz). Values measured with the PCM method vary from 3.11 GPa at 1 Hz to 3.3 GPa at  
26  
27 50 Hz. Values measured with both the flat punch and the Berkovich tip using the standard  
28  
29 CSM method at a frequency of 45 Hz are 3.70 and 3.74, respectively. The value of 45Hz was  
30  
31 chosen as it is the optimized frequency for the Nanoindenter<sup>®</sup> XP instrument. The values  
32  
33 experimentally determined for the elastic modulus of PS using the PCM method are in good  
34  
35 agreement with those presented in the literature for polystyrene, in the range of 3.0 to 3.6 GPa  
36  
37 (Brostow, 2007; Sperling, 2001). These results suggest that the PCM method is much more  
38  
39 robust than the standard CSM method to characterize viscoelastic samples in the frequency  
40  
41 domain, especially at lower frequencies.  
42  
43  
44  
45  
46  
47  
48  
49  
50  
51  
52  
53  
54  
55  
56  
57  
58  
59  
60  
61  
62  
63  
64  
65

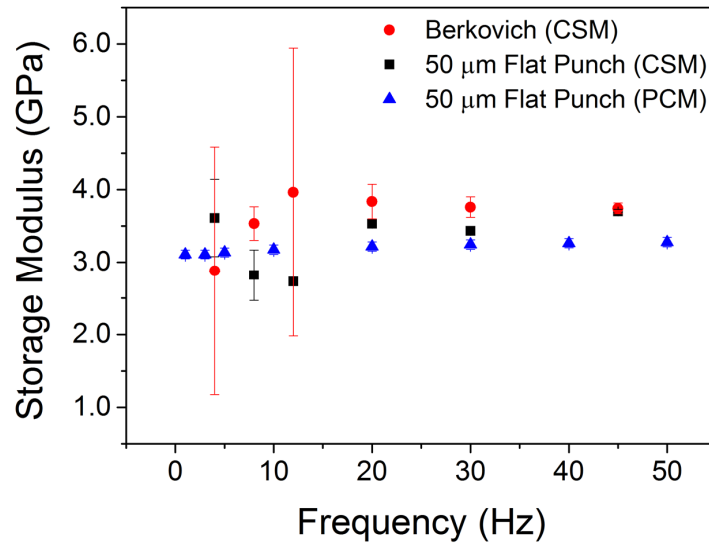


**Fig. 2:** Storage modulus as a function of frequency measured for the PS sample using different indenter tips and different nanoindentation methods. The error bars represent one standard deviation around the mean and can be obscured by the data points.

### 3.2 First tests on hydrogels: allowable creep rate issues

As indicated in Fig. 1, first tests on hydrogels using the Polymer Characterization Method were performed using an allowable creep rate of 0.3 nm/s. On the PS sample, this criterion was achieved in only 2 cycles of the stabilization routine. Nevertheless, a much longer time (usually longer than 3 h) was required for the contact to stabilize on hydrogels. Fig. 1(a) presents the load-time history of a single indentation experiment performed on a H30/700 sample, where the contact stabilization segment is indicated. Fig. 1(b) and (c) show the raw displacement as a function of time related to the contact stabilization routine of the experiment shown in Fig. 1(a). In contrast to the PS sample, even after 150 cycles of stabilization, the displacement rate of sample H30/700 appears to decrease only slightly despite the lower, constant load in each and every cycle. After ~2.5 h of stabilization, the measured creep rate was still 0.5 nm/s (see Fig. 1(c)).

The difference in the time needed for contact stabilization on polystyrene and hydrogels is consistent with results of force-relaxation experiments performed by Hu *et al.* (Hu *et al.*, 2011). The authors reported relaxation times in the order of hours for a swollen

1  
2  
3  
4 elastomer, while only tens of seconds were needed to relax the dried polymeric network. This  
5  
6 was attributed to the long time needed for water molecules to migrate into or out of the  
7  
8 polymeric network when load is applied to a gel (Hu et al., 2011).  
9

10  
11 In the present study, the main problem of the long stabilization time is that the  
12  
13 hydration method adopted in this study maintains the gels only laterally hydrated. The top  
14  
15 surface of the specimen is continuously in contact with air and subjected to drying. In order to  
16  
17 reduce the time for the contact stabilization procedure and measure the properties of the  
18  
19 hydrogels in the swollen state, a higher value of allowable creep rate (1.5 nm/s) was selected  
20  
21 for further experiments.  
22  
23

### 24 25 3.3 Storage Modulus ( $E'$ ) 26

27  
28 Fig. 3 shows the results of storage modulus as a function of frequency for the hydrogel  
29  
30 samples analyzed in this work. Data points represent the average of a minimum of 9  
31  
32 measurements.  $E'$  did not vary considerably with frequency for any of the hydrogel samples.  
33  
34 This indicates that the time-dependent behavior of these samples under dynamic loading is not  
35  
36 so marked and their mechanical response is similar to linear elasticity (at least in the  
37  
38 frequency range investigated in this work). This observation is consistent with measurements  
39  
40 performed by Roberts *et al.* (Roberts et al., 2011) on similar poly(ethylene glycol) (PEG)  
41  
42 hydrogels using dynamic unconfined compression in the frequency range of 0.01 to 10 Hz.  
43  
44  
45  
46  
47  
48  
49  
50  
51  
52  
53  
54  
55  
56  
57  
58  
59  
60  
61  
62  
63  
64  
65



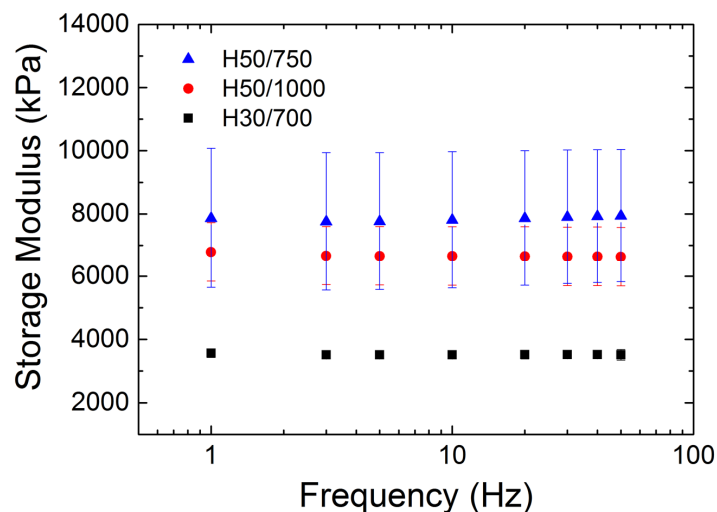


**Fig. 3:** Results of storage modulus measured by nanoindentation experiments for the three hydrogel samples analyzed in this work. The error bars span one standard deviation about the mean and can be obscured by the data points.

Also in agreement with other reports (Nayar et al., 2012; Oyen, 2013; Roberts et al., 2011; Shapiro and Oyen, 2014), the storage modulus of the hydrogel samples increased with increasing polymer concentration. This is evidenced by the lower  $E'$  obtained for sample H30/700 in comparison to those obtained for H50/750 and H50/1000 (see Table 2). In addition, all  $E'$  values measured in this study are of the same order of magnitude of values recently published for 50 wt% PEGDMA ( $\sim 4000$  kPa) (Shapiro and Oyen, 2014) and 30 wt% PEGDA ( $\sim 1700$  kPa) (Kohn and Ebenstein, 2013) hydrogels, both measured by spherical indentation.

The large standard deviation presented by the  $E'$  values measured for H50/750 and H50/1000 is potentially caused by the presence of inhomogeneities within the samples due to differences in the cross-linking density among different regions of the gel. In fact, the results of  $E'$  presented in Fig. 3 for the hydrogel H50/750 are the average of measurements performed in samples from two different batches of the same material (designated here A and B). When samples H50/750 A and B are analyzed separately,  $E'$  results look like those presented in Fig. 4. Nanoindentation experiments on the H30/700 and H50/1000 gels were all performed using a single sample batch.

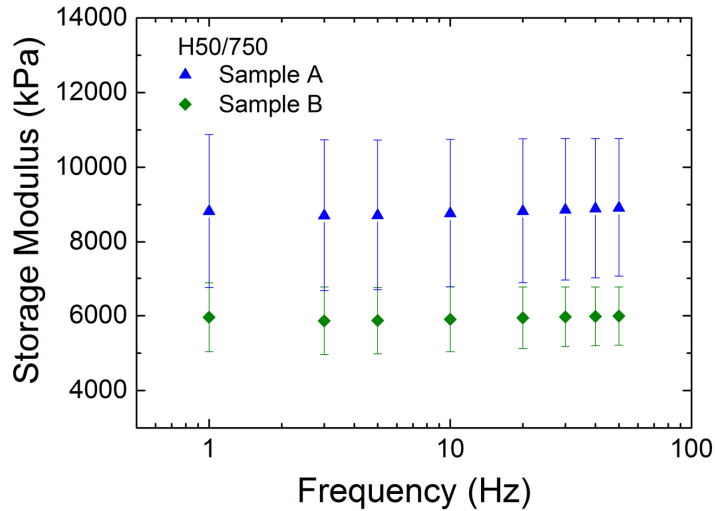


**Fig. 4:** Storage modulus results for the two different H50/750 hydrogel samples analyzed in this work.

### 3.4 Loss Modulus ( $E''$ ) and Loss Factor ( $\tan\delta$ )

Fig. 5(a) and (b) show the values of loss modulus and loss factor measured for all hydrogel samples analyzed in this work. Data points represent the average of at least 9 measurements. As observed in the results of storage modulus, a large scatter in the loss modulus was observed on the samples H50/750 and H50/1000, which may be attributed to inhomogeneities.

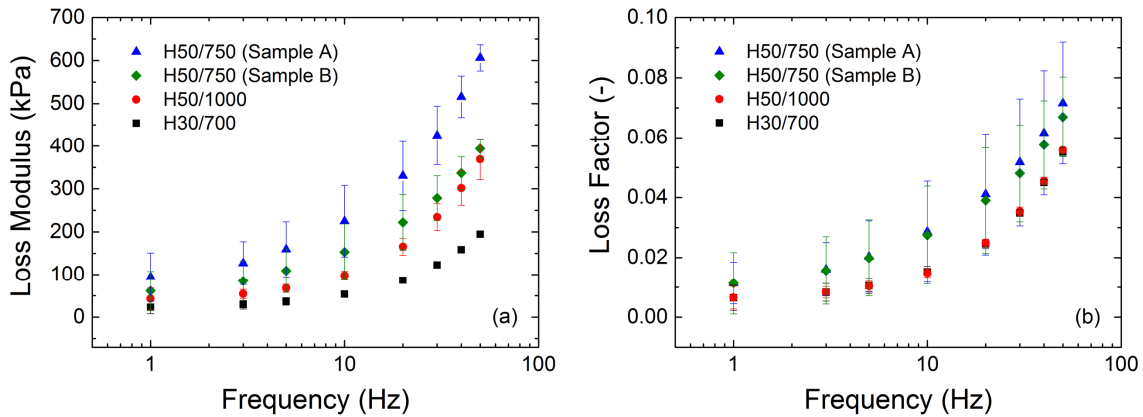


**Fig. 5:** Values of (a) loss modulus and (b) loss factor ( $\tan\delta$ ) for the hydrogel samples measured by nanoindentation in this study. The error bars span one standard deviation about the mean and can be obscured by the data points.

The magnitude of  $E''$  and  $\tan\delta$  increases over the frequency range of 1 to 50 Hz for all samples. As for the loss factor, the magnitude of samples H30/700 and H50/1000 are very

1  
2  
3  
4 similar to each other and, on average, are lower than that of H50/750 samples. Due to the  
5  
6 large standard deviation of the latter, a clear distinction among the different gels cannot be  
7  
8 made. Nevertheless, all measured values of loss factor are very small ( $\tan\delta < 0.1$ ), again  
9  
10 indicating the more elastic (than viscous) behavior of the gels analyzed here in the frequency  
11  
12 domain.  
13  
14

### 15 3.5 Comparison between nanoindentation and uniaxial compression

16  
17  
18 Table 2 shows results of elastic modulus obtained by the conventional compression  
19  
20 tests, together with those of storage modulus measured by nanoindentation at 50 Hz. Values  
21  
22 measured by nanoindentation are higher than those of uniaxial compression by a factor of 3.2  
23  
24 to 4.9 for all samples.  
25  
26

27  
28 **Table 2:** Storage moduli measured by uniaxial compression and nanoindentation for the hydrogels  
29 analyzed in this study. The nanoindentation values are for a frequency of 50 Hz.  
30

31 Testing 32 Technique	33 Storage Modulus (kPa)			
	H30/700	H50/1000	H50/750 A	H50/700 B
34 Uniaxial Compression	770	1350	1850	
35 Nanoindentation	3515 ± 168	6633 ± 940	8911 ± 1855	5989 ± 775

## 36 4. Discussion

### 37 4.1 Inhomogeneities in the hydrogel samples

38  
39  
40  
41  
42 The large standard deviations of  $E'$  and  $E''$  values obtained for samples H50-750 and  
43  
44 H50-1000 are attributed here to inhomogeneities in these materials. A factor that governs such  
45  
46 inhomogeneities is the solubility of the gel precursor in the solvent used for synthesis.  
47  
48 Methacrylate terminated OEGs (used in samples H50/750 and H50/1000) have a lower  
49  
50 solubility in water compared to that of acrylate groups (used in sample H30/700). This is due  
51  
52 to the more hydrophobic methacrylate backbone in relation to that of acrylate. In addition, 50  
53  
54 wt% OEGDMA was used to synthesize samples H50/750 and H50/1000, which is the  
55  
56 solubility limit of this polymer in water. As a consequence, the starting solutions used to  
57  
58  
59  
60  
61  
62  
63  
64  
65

1  
2  
3  
4 synthesize these gels had a high viscosity, leading to the formation of aggregates that resulted  
5  
6 in inhomogeneities during photopolymerization. Similar difficulties in gel preparation were  
7  
8 reported by Shapiro and Oyen (Shapiro and Oyen, 2014), who also mentioned the presence of  
9  
10 inhomogeneities in PEGDMA hydrogels produced with >50 wt% polymer concentration.  
11  
12 Sample H30/700, in turn, was synthesized with only 30 wt% OEGDA. This, associated with  
13  
14 the better solubility of the acrylate precursor in water, resulted in a lower viscos starting  
15  
16 solution and, therefore, in a better homogenization of the polymer into the solvent. As a  
17  
18 consequence, the material and its mechanical properties are more homogeneous. This is  
19  
20 confirmed by the low standard deviation of the  $E'$  and  $E''$  data measured for this sample. By  
21  
22 performing experiments with different punch geometries, thereby encompassing smaller or  
23  
24 larger volumes of material, it may be possible to provide experimental evidence to support  
25  
26 this hypothesis. This work aimed at determining the average viscoelastic properties of the  
27  
28 gels. Therefore, samples from different regions of the hydrogel plates were used for  
29  
30 nanoindentation experiments and the results averaged for each material. By focusing the  
31  
32 experiments on a small region of the gel and using a smaller punch radius, it may also be  
33  
34 possible to prove the feasibility of the PCM method to characterize inhomogeneities in  
35  
36 hydrogels or biological samples.  
37  
38  
39  
40  
41  
42

43 A second source for the large scatter in the mechanical properties of gels H50/750 and  
44  
45 H50/1000 is that the molecular weight of a polymer is given by a statistical probability  
46  
47 function, instead of by an absolute value. Therefore, the values of molecular weight presented  
48  
49 in Table 1 for the OEG-compounds (700, 750 and 1000 g/mol) are just the mean values of  
50  
51 probability distribution functions. The variations in values can be attributed to the  
52  
53 polydispersity of the oligo(ethylene glycol)s.  
54  
55

56 Fig. 4 evidences that the large scatter of the data presented in Fig. 3 for the sample  
57  
58 H50/750 is also in part due to differences in the mechanical behavior of the two different  
59  
60 sample batches tested (A and B). However, whether this different behavior was due to  
61  
62  
63  
64  
65

1  
2  
3  
4 variations in the molecular weight distribution or to some variation in the synthesis  
5  
6 parameters between the two batches is still unclear.  
7  
8

#### 9 10 *4.1 Transient creep behavior of hydrogels*

11  
12 When a load is applied to a hydrated material, not just the solid network deforms, but  
13 also a fluid flow is induced by the load (Oyen, 2013). The underlying mechanism for creep or  
14 stress relaxation differs, therefore, from that of a bulk viscoelastic material such as  
15 polystyrene. When a hydrogel is indented, the local compression load causes an instantaneous  
16 increase in pore pressure near the contact, which generates a pore pressure gradient within the  
17 matrix. To equilibrate this gradient, the fluid is induced to flow from the regions of higher  
18 pore pressure to those of lower pressure. Upon load removal, the fluid moves back into the  
19 matrix, and the material recovers its original form, like a fluid-filled sponge (Steck et al.,  
20 2003).  
21  
22  
23  
24  
25  
26  
27  
28  
29  
30  
31  
32

33 By the behavior shown in Fig. 1(b) and (c), the analyzed hydrogel seems to continue  
34 deforming, regardless the load applied to it, so that the contact stabilization routine continues  
35 extensively, without the achievement of an equilibrium. Due to the decrease in the applied  
36 load, the material does recover its form in each cycle (i.e., achieves the displacement target).  
37  
38 However, as soon as the load is held constant again, the material deforms further. In a  
39 parametric sense, the mechanical response of this hydrogel to an applied static load seems to  
40 be dominated by a dashpot, with no significant contribution from an elastic spring to the  
41 restoring capability of the sample. The behavior shown in Fig. 1(b) and (c) is probably  
42 dictated by the fluid flow within the matrix (i.e., poroelasticity), which seems to be induced  
43 even at very low applied loads, as long as there is a pressure gradient inside the matrix.  
44  
45  
46  
47  
48  
49  
50  
51  
52  
53  
54  
55  
56  
57  
58  
59  
60  
61  
62  
63  
64  
65

#### 4.2 Viscoelastic properties of hydrogels

The lower values of  $E'$  presented by the H30/700 sample in relation to the H50/750 and H50/1000 were expected, since the lower amount of OEG-diacrylate in the initial cross-linking solution leads to a higher degree of swelling after polymerization of the hydrogel and, therefore, to a more compliant behavior. This is in good agreement with recent results reported by Shapiro and Oyen (Shapiro and Oyen, 2014) and Roberts *et al.* (Roberts et al., 2011), who showed that the elastic modulus of PEG hydrogels increases with increasing the total polymer concentration.

Between samples H50/750 and H50/1000, the parameter dictating the mechanical properties is the different molecular weight of the OEG-dimethacrylates used to synthesize each sample. Cross-linking in these hydrogels occurs by reactions among the dimethacrylate end groups of different OEG molecules. A lower OEG molecular weight leads therefore to a higher density of cross-links. By increasing the cross-linking density, the pore size of the structure is reduced, leading to a reduction in the swelling degree and, consequently, to an increase in the polymer volume fraction in the swollen state. All these influencing factors lead to a stiffer behavior and should result in higher elastic modulus for the H50/750 gel in relation to that of H50/1000. However, in the tests performed in this study, although the average  $E'$  values of H50/750 were higher than those of the H50/1000, the results measured for the latter lie within the scatter band of the H50/750 sample, such that a clear discrimination between both materials cannot be made.

While the reason for the variation between samples H50/750 A and B is not fully understood, it is likely that this is due to differences in the mechanical behavior of the two samples rather than to inaccuracies in the nanoindentation method used. Supporting this conclusion are the  $E'$  values measured on sample H30/700, which presented a much higher repeatability among different tests, due to a higher homogeneity of the sample. If the scatter of the  $E'$  values observed in this study was due to some incapacity of this technique to

1  
2  
3  
4 characterize compliant materials, it would be expected that the largest variation of results  
5  
6 would be observed for the sample with the lowest elastic modulus, i.e. the H30/700. The fact  
7  
8 that the nanoindentation method used in this study was capable of measuring  $E'$  values in the  
9  
10 range of 3.4 to 3.7 MPa for this sample, with very low standard deviations (about  $\pm 0.134$   
11  
12 MPa), strongly supports our conclusion that the PCM method provides accurate  
13  
14 measurements of the mechanical properties of very compliant materials, such as hydrogels.  
15  
16

17  
18 The differences in mechanical response observed between the two H50/750 samples,  
19  
20 namely A and B, are therefore attributed to physical differences between the samples. After  
21  
22 testing the H50/750 A and B samples, and identifying the significant variation in moduli  
23  
24 between the two batches, it was recognized that the two batches of samples were prepared  
25  
26 separately, by two different people on different days. More importantly, the sample “age”,  
27  
28 distinguished here by the time between when the sample was prepared and when it was tested,  
29  
30 differed between the two batches by months; samples A and B were tested in the same week,  
31  
32 but sample B was received shortly before testing commenced while sample A had arrived  
33  
34 months prior to the establishment of the appropriate testing protocol. An aging study of PVA  
35  
36 hydrogels showed that the elastic modulus increases with aging time by a factor of 5 or 10  
37  
38 within the first month (Holloway et al., 2013).  
39  
40  
41  
42

43  
44 As defined by Eq. 3, the combination of low values of loss modulus with large values  
45  
46 of storage modulus leads to very low values of loss factor, as observed for all samples. Values  
47  
48 of  $\tan\delta$  were in the range of 0.01 to 0.06. According to Abdurrahmanoglu *et al.*  
49  
50 (Abdurrahmanoglu et al., 2009) and Okay and Oppermann (Okay and Oppermann, 2007), a  
51  
52 gel is considered strong when its storage modulus present low sensitivity for different  
53  
54 frequencies and the measured values of  $\tan\delta$  are in the order 0.01 (i.e.,  $E''$  is two orders of  
55  
56 magnitude lower than  $E'$ ). This means that the gel presents negligible viscous properties and,  
57  
58 in a parametric sense, its mechanical behavior is dominated by a spring. This seems to be  
59  
60 exactly the case of the OEG hydrogels analyzed in this study by dynamic nanoindentation.  
61  
62  
63  
64  
65

1  
2  
3  
4 Therefore, even though the creep behavior could not be completely settled in the  
5  
6 contact stabilization segment, the gels present a predominantly elastic behavior under  
7  
8 dynamic loads. This may be related to the fact that, under the application of a sinusoidal load,  
9  
10 the fluid does not have much time to flow through the pores of the structure, reducing the  
11  
12 contribution of poroelasticity to the time-dependent deformation. This emphasizes the  
13  
14 relevance of determining the mechanical properties of gels not only under static loading, but  
15  
16 also in the frequency domain.  
17  
18  
19  
20

#### 21 *4.4 Comparison between nanoindentation and uniaxial compression*

22

23 Measuring the elastic modulus of a viscoelastic material by analysing the slope of a  
24  
25 stress-strain curve can be very misleading, since the isolation of linear elastic behavior from  
26  
27 the time-dependent deformation is not possible or, at least, very complicated using a  
28  
29 monotonic loading method. This is one reason why dynamic techniques are widely preferred  
30  
31 by modelers and designers to characterize viscoelastic materials. The fact that the values  
32  
33 presented in Table 2 for the elastic modulus of the hydrogels as obtained through uniaxial  
34  
35 compression are lower than those measured by dynamic nanoindentation emphasizes the  
36  
37 difficulties of using a quasi-static test to measure the elastic response of time-dependent  
38  
39 materials. Using static loading for the characterization of hydrogels is only possible if stress  
40  
41 relaxation or creep experiments are performed, in which the instantaneous and equilibrium  
42  
43 moduli are characterized, together with deformation time constants (Oyen, 2014).  
44  
45  
46  
47  
48  
49

### 50 **5. Concluding remarks**

51

52 In this work, OEG-based hydrogels containing different polymer concentrations and  
53  
54 OEG molecular weights, as well as providing either a hydrophobic methacrylate or a less  
55  
56 hydrophobic acrylate backbone were characterized in the hydrated state using a new dynamic  
57  
58 nanoindentation testing method. This new polymer characterization method (PCM) was  
59  
60 shown to be a powerful tool to characterize the viscoelastic properties of soft materials with  
61  
62  
63  
64  
65



1  
2  
3  
4 elastic modulus in the range of a few MPa. Experimental verification of the test method was  
5  
6 conducted on a standard polystyrene (PS) sample and the measured storage modulus,  $E'$ , was  
7  
8 found to be in excellent agreement with the literature value. Furthermore, results from the  
9  
10 PCM method on PS showed greater reproducibility than results from standard CSM  
11  
12 indentation experiments using both Berkovich and flat punch indenters.  
13  
14

15 Values of  $E'$  measured for H30/700 were lower than those measured for the H50/750  
16  
17 and H50/1000, due to its lower polymer concentration and, therefore, higher water content in  
18  
19 the swollen state (higher swelling degree). The influence of the molecular weight in the  
20  
21 mechanical properties of H50/750 and H50/1000 could however not be clearly detected due to  
22  
23 different mechanical responses of the two H50/750 sample batches analyzed in this work.  
24  
25 While aging effects are not well understood, they have been observed on samples H50/750  
26  
27 and could be critical to the function of a hydrogel in the field. The use of the PCM method  
28  
29 and could be critical to the function of a hydrogel in the field. The use of the PCM method  
30  
31 offers a strong advantage over other characterization techniques for assessing ageing effects;  
32  
33 the method requires only a small volume of material, is rather non-destructive, requires little  
34  
35 sample preparation and can be carried out within an aqueous environment. A systematic  
36  
37 investigation of the various effects on hydrogel mechanical response can be readily carried  
38  
39 out on the influences of ageing, pH, chemical sensitivity, etc. for a single sample,  
40  
41 circumventing the usual issues of sample to sample variations.  
42  
43  
44

45 Values of  $E'$  measured for all hydrogel samples did not vary over the range of  
46  
47 frequencies analyzed in this study. Additionally, the values of  $E''$  were two orders of  
48  
49 magnitude lower than the  $E'$  ( $\tan\delta < 0.1$ ) for all samples, as is characteristic of strong gels  
50  
51 with negligible viscous behavior.  
52  
53

54 Finally, it is important to note that the  $E'$  values measured are in the range of values  
55  
56 measured by dynamic nanoindentation on porcine cartilage (~3-9 MPa between 10 and 50  
57  
58 Hz) (Franke et al., 2011), suggesting that the OEG hydrogels analyzed in this work are good  
59  
60 candidates for applications in cartilage regeneration.  
61  
62  
63  
64  
65

1  
2  
3  
4 **References**  
5

- 6  
7 Abdurrahmanoglu, S., Can, V., Okay, O., 2009. Design of high-toughness polyacrylamide  
8 hydrogels by hydrophobic modification. *Polymer* 50, 5449–5455.  
9
- 10 Ahearne, M., Yang, Y., El Haj, A.J., Then, K.Y., Liu, K.-K., 2005. Characterizing the  
11 viscoelastic properties of thin hydrogel-based constructs for tissue engineering  
12 applications. *Journal of the Royal Society Interface* 2, 455-463.  
13
- 14 Anseth, K.S., Bowman, C.N., Brannon-Peppas, L., 1996. Mechanical properties of hydrogels  
15 and their experimental determination. *Biomaterials* 17, 1647-1657.  
16
- 17 Brostow, W., 2007. Mechanical properties, in: James, E.M. (Ed.), *Physical Properties of*  
18 *Polymers Handbook*, 2 ed. Springer Science & Business Media, New York, p. 1076.  
19
- 20 Cauich-Rodriguez, J.V., Deb, S., Smith, R., 1996. Dynamic mechanical characterization of  
21 hydrogel blends of poly(vinyl alcohol-vinyl acetate) with poly(acrylic acid) or  
22 poly(vinyl pyrrolidone). *Journal of Materials Science: Materials in Medicine* 7, 349-  
23 353.  
24
- 25 Deuschle, J., 2008. *Mechanics of soft polymer indentation*. University of Stuttgart, Stuttgart,  
26 p. 189.  
27
- 28 Ebenstein, D.M., Pruitt, L.A., 2004. Nanoindentation of soft hydrated materials for  
29 application to vascular tissues. *Journal of Biomedical Materials Research* 69A, 222-232.  
30
- 31 Ebenstein, D.M., Pruitt, L.A., 2006. Nanoindentation of biological materials. *Nanotoday* 1,  
32 26-33.  
33
- 34 Engler, A.J., Sen, S., Sweeney, H.L., Discher, D.E., 2006. Matrix Elasticity Directs Stem Cell  
35 Lineage Specification. 126, 677-689.  
36
- 37 Franke, O., Durst, K., Maier, V., Göken, M., Birkholz, T., Schneider, H., Hennig, F., Gelse,  
38 K., 2007. Mechanical properties of hyaline and repair cartilage studied by  
39 nanoindentation. *Acta Biomaterialia* 3, 873-881.  
40
- 41 Franke, O., Göken, M., Hodge, A.M., 2008. The nanoindentation of soft tissue: Current and  
42 developing approaches. *Biological Materials Science* 60, 49-53.  
43
- 44 Franke, O., Göken, M., Meyers, M.A., Durst, K., Hodge, A.M., 2011. Dynamic  
45 nanoindentation of articular porcine cartilage. *Materials Science and Engineering C* 31,  
46 789-795.  
47
- 48 Galli, M., Comley, K.S.C., Shean, A.V., Oyen, M.L., 2008. Viscoelastic and poroelastic  
49 mechanical characterization of hydrated gels. *Journal of Materials Research* 24, 973-  
50 979.  
51
- 52 Gläber, S., Stampfl, J., Koch, T., Seidler, S., Schüller, G., Redl, H., Juras, V., Trattnig, S.,  
53 Weidish, R., 2009. Determination of the viscoelastic properties of hydrogels on  
54 polyethylene glycol diacrylate (PEG-DA) and human articular cartilage. *Internal Journal*  
55 *of Materials Engineering Innovation* 1, 3-20.  
56  
57  
58  
59  
60  
61  
62  
63  
64  
65

- 1  
2  
3  
4 Herbert, E.G., Oliver, W.C., Lumsdaine, A., Pharr, G.M., 2009. Measuring the constitutive  
5 behavior of viscoelastic solids in the time and frequency domain using flat punch  
6 nanoindentation. *Journal of Materials Research* 24, 626-637.  
7
- 8 Herbert, E.G., Oliver, W.C., Pharr, G.M., 2008. Nanoindentation and dynamic  
9 characterization of viscoelastic solids. *Journal of Physics D: Applied Physics* 41, 1-9.  
10
- 11 Holloway, J.L., Lowman, A.M., Palmese, G.R., 2013. The role of crystallization and phase  
12 separation in the formation of physically cross-linked PVA hydrogels. *Soft Matter* 9,  
13 826-833.  
14
- 15 Hu, Y., Chen, X., Whitesides, G.M., Vlassak, J.J., Suo, Z., 2011. Indentation of  
16 polydimethylsiloxane submerged in organic solvents. *Journal of Materials Research* 26,  
17 785-795.  
18
- 19 Hu, Y., You, J.-O., Auguste, D.T., Suo, Z., Vlassak, J.J., 2012. Indentation: A simple,  
20 nondestructive method for characterising the mechanical and transport properties of pH-  
21 sensitive hydrogels. *Journal of Materials Research* 27, 152-160.  
22
- 23 Iza, M., Stoianovici, G., Viora, L., Grossiord, J.L., Couarraze, G., 1998. Hydrogels of  
24 poly(ethylene glycol): mechanical characterization and release of a model drug. *Journal*  
25 *of Controlled Release* 52, 41-51.  
26
- 27 Kaufman, J.D., Klapperich, C.M., 2009. Surface detection errors cause overestimation of the  
28 modulus in nanoindentation on soft materials. *Journal of Mechanical Behavior of*  
29 *Biomedical Materials* 2, 312-317.  
30
- 31 Kaufman, J.D., Miller, G.J., Morgan, E.F., C.M., K., 2008. Time-dependent mechanical  
32 characterization of poly(2-hydroxyethyl methacrylate) hydrogels using nanoindentation  
33 and unconfined compression. *Journal of Materials Research* 23, 1472-1481.  
34
- 35 Kohn, J.C., Ebenstein, D.M., 2013. Eliminating adhesion errors in nanoindentation of  
36 compliant polymers and hydrogels. *Journal of the Mechanical Behavior of Biomedical*  
37 *Materials* 20, 316-326.  
38
- 39 Lin, C.-C., Anseth, K.S., 2009. PEG hydrogels for the controlled release of biomolecules in  
40 regenerative medicine. *Pharmaceutical Research* 26, 631-643.  
41
- 42 Liu, K., VanLandingham, M.R., Ovaert, T.C., 2009. Mechanical characterization of soft  
43 viscoelastic gels via indentation and optimization-based inverse finite elements analysis.  
44 *Journal of Mechanical Behavior of Biomedical Materials* 2.  
45
- 46 Lum, L., Elisseeff, J., 2003. Injectable hydrogels for cartilage tissue engineering, in:  
47 Ashammakhi, N., Ferretti, P. (Eds.), *Topics in Tissue Engineering*. University of Oulu.  
48
- 49 Nayar, V.T., Weiland, J.D., Nelson, C.S., Hodge, A.M., 2012. Elastic and viscoelastic  
50 characterization of agar. *Journal of the Mechanical Behavior of Biomedical Materials* 7,  
51 60-68.  
52
- 53 Okay, O., Oppermann, W., 2007. Polyacrylamine-clay nanocomposite hydrogel: rheological  
54 and light scattering characterization. *Macromolecules* 40, 3378-3387.  
55  
56  
57  
58  
59  
60  
61  
62  
63  
64  
65

- 1  
2  
3  
4 Oliver, W.C., Pharr, G.M., 1992. An improved technique for determining hardness and elastic  
5 modulus using load and displacement sensing indentation experiments. *Journal of*  
6 *Materials Research* 7, 1564-1583.  
7  
8 Oliver, W.C., Pharr, G.M., 2004. Measurement of hardness and elastic modulus by  
9 instrumented indentation: Advances in understanding and refinements to methodology.  
10 *Journal of Materials Research* 19, 3-20.  
11  
12 Oyen, M.L., 2006. Analytical techniques for indentation of viscoelastic materials.  
13 *Philosophical Magazine* 83, 1-17.  
14  
15 Oyen, M.L., 2007. Viscoelastic effects in small-scale indentation of biological materials.  
16 *International Journal of Surface Science and Engineering* 1.  
17  
18 Oyen, M.L., 2013. Nanoindentation of biological and biomimetic materials. *Experimental*  
19 *Techniques* 37, 73-87.  
20  
21 Oyen, M.L., 2014. Mechanical characterisation of hydrogel materials. *International Materials*  
22 *Reviews* 59, 44-59.  
23  
24 Oyen, M.L., Bembey, A.K., Bushby, A.J., 2007. Poroelastic indentation analysis for hydrated  
25 biological tissues, in: Viney, C., Katti, K., Hellmich, C., Wegst, U. (Eds.), 2006 MRS  
26 Fall Meeting: Symposium DD - Mechanics of Biological and Bio-Inspired Materials.  
27  
28 Oyen, M.L., Cook, R.F., 2009. A practical guide for analysis of nanoindentation data *Journal*  
29 *of Mechanical Behavior of Biomedical Materials* 2, 396-407.  
30  
31 Peppas, N.A., Huang, Y., Torres-Hugo, M., Ward, J.H., Zhang, J., 2000. Physicochemical  
32 foundation and structural design of hydrogels in medicine and biology. *Annu. Rev.*  
33 *Biomedical Eng.* 02, 9-29.  
34  
35 Peppas, N.A., Merrill, E.W., 1977. Crosslinked poly(vinyl alcohol) hydrogels as swollen  
36 elastic networks. *Journal of Applied Polymer Science* 21, 1763-1770.  
37  
38 Roberts, J.J., Earnshaw, A., Ferguson, V.L., Bryant, S.J., 2011. Comparative study of the  
39 viscoelastic mechanical behavior of agarose and poly(ethylene glycol) hydrogels.  
40 *Journal of Biomedical Materials Research Part B: Applied Biomaterials* 99B, 158-169.  
41  
42 Shapiro, J.M., Oyen, M.L., 2014. Viscoelastic analysis of single-component and composite  
43 PEG and alginate hydrogels. *Acta Mechanica Sinica* 30, 7-14.  
44  
45 Sperling, L.H., 2001. *Introduction to Physical Polymer Science*, 3 ed. John Wiley and Sons,  
46 Inc., New York.  
47  
48 Steck, R., Niederer, P., Knothe Tate, M.L., 2003. Fluid flows through anisotropic, poroelastic  
49 bone models in the opposite direction to that through analogous isotropic models,  
50 Summer Bioengineering Conference, Sonesta Beach Resort in Key Biscayne, Florida.  
51  
52 Thomas, J., Gomes, K., Lowman, A., Marcolongo, M., 2004. The effect of dehydration  
53 history on PVA/PVP hydrogels for nucleus pulposus replacement. *Journal of*  
54 *Biomedical Materials Research Part B: Applied Biomaterials* 69B, 135-140.  
55  
56  
57  
58  
59  
60  
61  
62  
63  
64  
65

1  
2  
3  
4  
5  
6  
7  
8  
9  
10  
11  
12  
13  
14  
15  
16  
17  
18  
19  
20  
21  
22  
23  
24  
25  
26  
27  
28  
29  
30  
31  
32  
33  
34  
35  
36  
37  
38  
39  
40  
41  
42  
43  
44  
45  
46  
47  
48  
49  
50  
51  
52  
53  
54  
55  
56  
57  
58  
59  
60  
61  
62  
63  
64  
65

Tyrrel, J.W.G., Attard, P., 2003. Viscoelastic study using an atomic force microscope modified to operate as a nanorheometer. *Langmuir* 19, 5254-5260.

White, C.C., VanLandingham, M.R., Drzal, P.L., Chang, N.-K., Chang, S.-H., 2005. Viscoelastic characterization of polymers using instrumented indentation. II. Dynamic Testing. *Journal of Polymer Science Part B: Polymer Physics* 43, 1812-1824.